Imaging the Fate of Implanted Bone Marrow Stromal Cells Labeled With Superparamagnetic Nanoparticles

Pavla Jendelová,[1,3,4] Vít Herynek,[2] Jane DeCroos,[1,3] Kateřina Glogarová,[1,3] Benita Andersson,[3,5] Milan Hájek,[2] and Eva Syková[1,3,4]*

Bone marrow stromal cells (MSCs) are pluripotent progenitor cells that have the capacity to migrate toward lesions and induce or facilitate site-dependent differentiation in response to environmental signals. In animals with a cortical photochemical lesion, the fate of rat MSCs colabeled with magnetic iron-oxide nanoparticles (Endorem®) and bromodeoxyuridine (BrdU) was studied. MSCs were either grafted intracerebrally into the contralateral hemisphere of adult rat brain or injected intravenously. In vivo MRI was used to track their fate; Prussian blue staining and transmission electron microscopy (TEM) confirmed the presence of iron-oxide nanoparticles inside the cells. During the first week posttransplantation, the transplanted cells migrated to the lesion site and populated the border zone of the damaged cortical tissue. The implanted cells were visible on MR images as a hypointense area at the injection site and in the lesion. The hypointense signal persisted for more than 50 days. The presence of BrdU-positive and iron-containing cells was confirmed by subsequent histological staining. Three to 4 weeks after injection, <3% of MSCs around the lesion expressed the neuronal marker NeuN. Our study demonstrates that a commercially available contrast agent can be used as a marker for the long-term noninvasive MR tracking of implanted cells. Magn Reson Med 50:767–776, 2003. © 2003 Wiley-Liss, Inc.

Key words: cell transplantation; magnetic resonance; stem cells; contrast agents; injury

The adult central nervous system (CNS) possesses a limited capacity for regeneration, and therefore the prospects for recovery from traumatic injury, ischemia, or degenerative disease are generally grim. However, new possibilities for repairing the nervous system have arisen since the discovery of stem cells, which can differentiate into nerve cells. Recent studies have demonstrated that different types of stem cells can be transplanted successfully in animal models of disease or injury (for reviews, see Refs. 1–3). In cell therapy, bone marrow stromal cells (MSCs) have some advantages over other sources of cells: they are relatively easy to isolate (from bone marrow) and can be used in autologous transplantation protocols, and have already been approved for the treatment of hematopoietic diseases. MSCs are nonhematopoietic stem cells that are capable of self-renewal and can differentiate in culture into osteoblasts, chondrocytes, adipocytes, and myoblasts (4). After MSCs are transplanted into the brain, they respond to intrinsic signals and differentiate in vivo into astrocytes and even neurons (4,5). MSCs have also been reported to bridge the epicenter of a spinal cord injury (6). Various routes for MSC administration have been tested. Hofstetter et al. (6) injected the cells directly into the damaged area of the spinal cord, and to both edges of the lesion. Kopen et al. (5) injected MSCs into the lateral ventricle of neonatal mice. These cells then migrated throughout the forebrain and cerebellum, including the striatum, the molecular layer of the hippocampus, the olfactory bulb, and the internal granular layer of the cerebellum. Lu et al. (7,8) transplanted MSCs either directly into the striatum and cortex or intravenously into rats exposed to brain injury and focal cerebral ischemia. In the majority of such experiments, the donor cells were labeled before transplantation with bromodeoxyuridine (BrdU), green fluorescent protein (GFP), or lacZ (5,7–10). After a certain time, the host organism was killed and the position of the transplanted cells was evaluated by microscopic analysis. However, histological evaluation does not provide information about the dynamics of the migration of the transplanted stem cells in the host organism.

Cells that are magnetically labeled with superparamagnetic iron-oxide particles (SPIO) can be observed in vivo using MRI. The first studies of imaging cell transplants labeled by superparamagnetic (SPM) contrast agents in rat brains were reported in 1992 (11,12). Different iron-oxide nanoparticles coated by dextran were tested. For example, BMS180549 was successfully used to label T-cells (13), and it was proven that MRI could be used for the dynamic in vivo tracking of labeled cells (14). The greatest progress was achieved with dextran-coated monocrystalline iron-oxide nanoparticles (MION), the properties of which have been broadly studied (15–17). Different derivatives of MION were used for cell labeling to track migration (e.g., the migration of MION-labeled oligodendrocyte progenitors was shown (18)). Superparamagnetic MION are widely used because of their small size (4–7 nm) and their known magnetic and biochemical properties, which enable the contrast agent to be shuttled into the cell. Dendrimer-encapsulated superparamagnetic iron oxides have been used for labeling and in vivo tracking of stem cells

[1]Center for Cell Therapy and Tissue Repair, Charles University, Second Medical Faculty, Prague, Czech Republic.

[2]MR Unit, Radiology Department, Institute for Clinical and Experimental Medicine, Prague, Czech Republic.

[3]Institute of Experimental Medicine, Academy of Sciences of Czech Republic, Prague, Czech Republic.

[4]Department of Neuroscience, Charles University, Second Medical Faculty, Prague, Czech Republic.

[5]Department of Clinical Neuroscience, Karolinska Institutet, Stockholm, Sweden.

Grant sponsor: Ministry of Education, Sports and Youth of the Czech Republic; Grant numbers: LN 00A065; J13/98:11130004; Grant sponsor: Academy of Sciences of the Czech Republic; Grant number: AVOZ5039906; Grant sponsor: Grant Agency of the Czech Republic; Grant number: 304/03/1189; Grant sponsor: Ministry of Health of the Czech Republic; Grant number: L17/98:00023001.

*Correspondence to: Prof. Eva Syková, M.D., D.Sc., Institute of Experimental Medicine ASCR, Vídeňská 1083, 140 20 Prague 4, Czech Republic. E-mail: sykova@biomed.cas.cz

Received 13 March 2003; revised 16 May 2003; accepted 12 June 2003.

DOI 10.1002/mrm.10585

Published online in Wiley InterScience (www.interscience.wiley.com).

(19). Recently, immortalized cells from the MHP36 hippocampal cell line labeled in vitro with gadolinium rhodamine dextran (GRID) were tracked in ischemia-damaged rat hippocampus in perfused brain ex vivo (20). A study in which embryonic stem cells were labeled in vitro with the MR contrast agent Sinerem®, using a lipofection procedure, successfully showed the migration of labeled cells into focal cerebral ischemic lesions evoked by middle cerebral artery occlusion (21).

In the current study we investigated the fate of implanted rat MSCs labeled with iron-oxide nanoparticles and mouse C3H MSCs implanted in intact rats or rats with cortical photochemical lesions. To monitor the behavior and migration of grafted cells in vivo by MRI, we chose to label the cells with Endorem® (Guerbet, France). This commercially available contrast agent is based on dextran-coated iron-oxide nanoparticles, and has been approved for human use. Endorem® is available in the form of an aqueous colloid. The crystal size varies from 4.3 to 5.6 nm, and the whole particle size is 150 nm (22). Their strong T_1 and T_2 effects are characterized by high relaxivities (R_1 = 23 $mM^{-1}s^{-1}$, R_2 = 100 $mM^{-1}s^{-1}$ at 20 MHz), which are on the same order as those of MION-based contrast agents. However, the relaxivity related to iron content is lower, because iron does not create monocrystals inside the Endorem® particles, and thus the SPM moment is lower.

METHODS

Cell Cultures and Labeling With Endorem®

To isolate the rat MSCs, femurs were dissected from 4-week-old Wistar rats. The ends of the bones were cut, and the marrow was extruded with 5 mL of DMEM using a needle and syringe. Marrow cells were plated on an 80-cm^2 tissue culture flask in DMEM/10% FBS with 100 U/mL penicillin and 100 U/mL streptomycin. After 24 hr, the nonadherent cells were removed by replacing the medium. The medium was replaced every 2–3 days as the cells grew to confluence. The cells were lifted by incubation with 0.25% trypsin. After six to 10 passages, the cells were implanted as a cell suspension. Mouse C3H MSCs were isolated from femurs of the inbred mouse strain C3H/N. The C3H MSCs were expanded in vitro under the same conditions as the rat MSCs.

An Endorem® suspension (200 μl per 20 mL of culture medium, i.e., 2.2 mg of iron) was added to the rat MSC culture 5 days prior to transplantation. After 72 hr the contrast agent was washed out. The rat MSCs were colabeled with 5 μM BrdU (Sigma) 24 hr prior to transplantation.

Experimental Animals

Male Wistar rats (6–8 weeks old) were used throughout the study. The animals were divided into the following groups: 1) rats with Endorem®- and BrdU-colabeled rat MSCs grafted into their intact brain (N = 10) or injected intravenously (N = 6); 2) rats with a cortical photochemical lesion and with contralaterally grafted Endorem®- and BrdU-colabeled rat MSCs (N = 15); 3) Endorem®-labeled mouse C3H MSCs (N = 5); 4) rats with a lesion and with Endorem®- and BrdU-colabeled rat MSCs administered intravenously (N = 12); and 5) rats with a lesion injected with phosphate-buffered saline (PBS) into the contralateral hemisphere or intravenously (N = 6).

All experiments were carried out in accordance with the European Communities Council Directive of 24 November 1986 (86/609/EEC).

Photochemical Lesions

We used a photochemical lesion as a model of thrombotic stroke (23). The model uses a photochemical reaction in vivo to induce a thrombosis leading to a cerebral infarction. The method is virtually noninvasive because the skull is translucent for light at 560 nm, which is the wavelength used for inducing the photochemical reaction. The rats were anesthetized by isoflorane (2% isoflorane in air). Rose Bengal, a potent photosensitizing dye, was injected intravenously into the femoral vein (1 mg/100 g). A 1 × 2 mm area of the skull above the right cortex was exposed to the light from a halogen lamp for 10 min, while the rest of the skull was shielded with aluminium foil. Rose Bengal absorbs light at 560 nm. It is excited and subsequently generates singlet molecular oxygen (through active quenching of the lowest triplet state by molecular oxygen). Thus it has the ability to induce photoperoxidative reactions. Damage to lipid membranes may provide an initial stimulus for platelet adhesion and subsequent aggregation, leading to thrombosis and infarction within 1 hr (23). The formation of thrombotic plugs and adjacent red blood cell stasis within pial and parenchymal vessels is thus observed within the irradiated zone. The rats were returned to their cages and left to recover.

Grafting of Marrow Stromal Cells

The rats were anesthetized with isoflorane 24 hr after the photochemical lesion developed, and were mounted in a stereotactic frame. Using an aseptic technique, a burr hole (1 mm) was made on the left side of the skull to expose the dura overlying the left cortex. Cells (3×10^5) were suspended in 3 μL of PBS and slowly injected over a 10-min period by a Hamilton syringe into the contralateral hemisphere AP = –1 mm, ML = 2.5 mm, and DV = 3.5 mm from the bregma (based on the atlas of Paxinos et al. (24)). The opening was closed by bone wax, and the skin was sutured. Approximately 2×10^6 cells in 0.5 mL PBS were injected intravenously into the femoral vein. The vein was compressed for a short time to reduce bleeding, and the wound was sutured. An immunosuppressive (Depo-Medrol®; UpJohn) was administered weekly.

MRI

MR images were obtained using a 4.7 T Bruker spectrometer equipped with an in-house-made surface coil. The rats were anesthetized by passive inhalation of 1.5–2% isoflorane in air. Breathing was monitored during the measurements. Single sagittal, coronal, and transversal images were obtained by a fast gradient-echo sequence to localize the subsequent T_2-weighted transversal images, as measured by a standard turbo spin-echo sequence. The sequence parameters were: repetition time (TR) = 2000 ms, effective echo time (TE) = 42.5 ms, turbo factor = 4,

number of acquisitions (AC) = 16, field of view (FOV) = 3.5 cm, matrix = 256 × 256, slice thickness = 0.5 mm, and slice separation = 1 mm. Two sets of interleaved transversal images were measured to cover the whole brain.

Phantoms containing labeled cells were measured by a similar sequence with different geometry: FOV= 6 cm, matrix = 256 × 256, and slice thickness = 1 mm. In the phantoms, only one slice was measured.

Histology and Immunohistochemistry

The rats were killed 2–7 weeks after transplantation. The anesthetized animals were perfused with 4% paraformaldehyde in 0.1 M PBS (pH 7.4). Fixed brains were dissected and immersed in PBS with 30% sucrose. Frozen coronal sections (40 μm) were cut through the areas of interest.

Transplanted cells were detected by staining for iron to produce ferric ferrocyanide (Prussian blue) and by anti-BrdU staining using a monoclonal antibody (Roche). As a secondary antibody, goat anti-mouse IgG Alexa 594 (Molecular Probes) was used. To visualize the possible colocalization of BrdU and cell-type-specific markers in the same cells, double staining was employed. Sections were incubated with cell-type-specific antibodies directed against a neuronal nuclear antigen (NeuN), dilution 1:100 (Chemicon), or against glial fibrilary acidic protein (GFAP) for identifying astrocytes, dilution 1:2500 (DAKO). Each coronal section was also incubated with monoclonal anti-BrdU, as described above. A fluorescein-conjugated secondary antibody (goat anti-mouse IgG Alexa 488) was used as the second label in the double-staining experiments. Mouse C3H MSCs were detected using a fluorescent-labeled monoclonal antibody (a gift from Prof. M. Kusakabe, Tsukuba Life Science Center, Tsukuba, Japan) recognizing a C3H-specific alloantigen, CSA (C3H strain-specific antigen (25)).

Electron Microscopy

For the electron microscopy examination, the MSCs were fixed at +4°C in 2.5% buffered glutaraldehyde for 1 hr, followed by 1% osmium tetroxide for 2 hr. The cells were dehydrated in ascending concentrations of ethanol, immersed in propylene-oxide, and embedded in the resin Epon 812 (Agar Scientific Ltd.; Standsted, UK). The samples were cut in ultrathin sections (~60 nm). These sections were contrasted with 4% uranyl acetate and Reynold's lead citrate, and examined in a Philips Morgagni 268 electron microscope.

Iron Content Quantitative Analysis

The amount of iron present in the cells was determined by spectrophotometry after mineralization. First, 2-ml samples containing 16.1 million cells were mineralized after the addition of 5 mL HNO_3 and 1 mL H_2O_2 in an ETHOS 900 (Millestone, Sydney, Australia) microwave mineralizator. Deionized water was added to reach a total volume of 100 mL. The iron content was determined using a Spectroflame M120S (Spectro Inc., Littleton, MA) calibrated in a standard solution of Astasol (Analytika Ltd., Prague, Czech Republic). The measurements were repeated four times, and the average mean value was determined.

RESULTS

Iron-Oxide-Labeled MSCs in Culture

By the use of an optical microscope (Axioskop, Zeiss) with phase contrast, the iron-oxide nanoparticles in MSCs in culture were observed as dark dots. Iron inside the cells was visualized by Prussian blue staining (Fig. 1). Transmission electron microscopy (TEM) confirmed the presence of 20–30 iron-oxide particles inside the cell, observed as endoplasmatic reticulum membrane-bound clusters within the cell cytoplasm (Fig. 1b). Vesicles containing Fe particles surrounded by a membrane indicated an endocytotic process of Fe uptake. The clusters were found in samples incubated for 48–72 hr; 24-hr incubation did not result in sufficient incorporation of iron into all of the cells. The mean iron concentration in a 2-mL sample containing 16.1 million cells was 141 μg/mL, which corresponds to an average value of 17.5 pg of iron per cell. After the Endorem® was washed out of the culture medium, the cells were colabeled with BrdU. Since BrdU is incorporated only into proliferating cells, double staining for BrdU and Prussian blue shows that iron-oxide-containing cells are viable. The Endorem®- and BrdU-colabeled cells were often observed dividing (Fig. 1c–e), and cells in culture remained viable at least for 10 consecutive passages (the length of the maximum observation period).

Fate of Grafted MSCs

In rats without a photochemical lesion (group 1), grafted MSCs survived in the brain; however, they did not migrate outside of the needle track. In a group of intact animals with rat MSCs injected intravenously, no cells were found in the brain parenchyma (apparently because they did not cross the blood–brain barrier). BrdU-positive cells were detected only in some of the brain capillaries.

When rat MSCs were injected into rats with a cortical photochemical lesion (groups 2 and 4), we found a massive migration of Endorem®/BrdU-labeled cells into the lesion site regardless of the route of administration (direct injection into the contralateral hemisphere or intravenous injection; Figs. 2a–c and 3a–d). From the contralateral hemisphere, the cells migrated along the corpus callosum. The cells massively populated the border zone of the damaged cortical tissue, and were localized in the injured tissue around the necrotic part of the photochemical lesion. No anti-BrdU-stained cells were found in brain regions other than the lesion. Only a few (<3%) of the cells that migrated into the lesion expressed the neuronal marker NeuN (Fig. 2d–f) when they were tested 28 days postimplantation. No GFAP-positive cells were found in the lesion.

To exclude the possibility that the BrdU from the implanted cells was taken up by macrophages (26), we grafted Endorem®-labeled mouse C3H MSCs (group 3) into the contralateral hemisphere. The mouse MSCs migrated into the lesion in the same manner and numbers as did the Endorem®/BrdU-colabeled rat MSCs (Fig. 2g–i). As the anti-CSA antibody recognizes only a C3H-specific alloantigen (C3H strain-specific antigen), we can be certain that the positively-stained cells, as well as the Prussian blue-

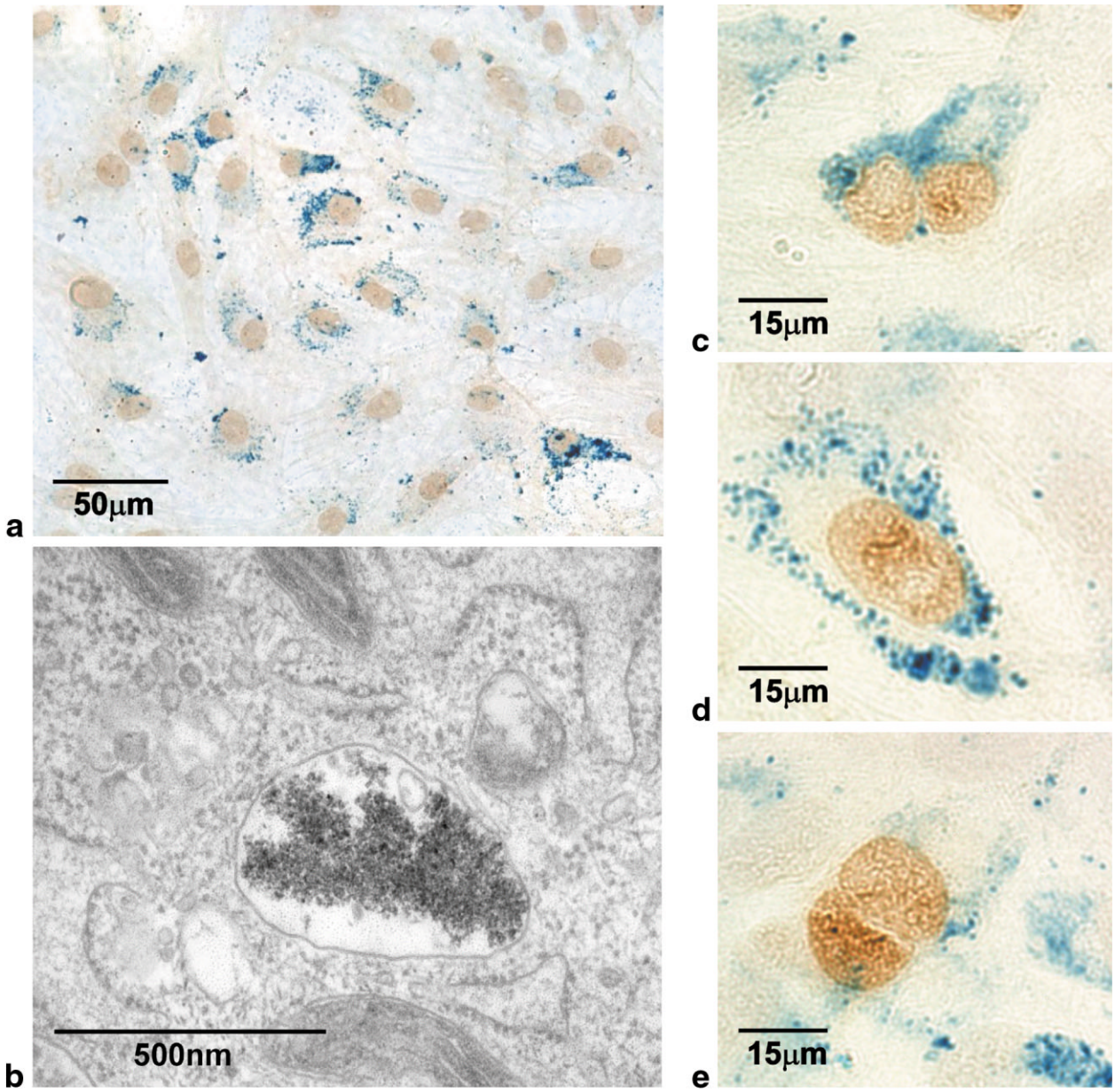

FIG. 1. MSC labeling with iron-oxide nanoparticles. **a:** Cells in culture labeled with BrdU (brown), containing the contrast agent Endorem® (Prussian blue staining). **b:** Transmission electron microphotograph showing a cluster of iron particles surrounded by a cell membrane, confirming the presence of iron inside the cell. **c–e:** Cells labeled with Endorem® undergoing cell division, confirming that incorporation of Endorem® does not adversely affect cell viability (anti-BrdU and Prussian blue staining).

stained cells, were only mouse C3H MSCs and not host macrophages. We did not find any positive staining for BrdU in lesioned control rats.

In Vitro MRI Detection of MSCs

To check the sensitivity of the MRI technique and to mimic signal behavior in the brain tissue, we performed in vitro imaging of labeled cells. Rat MSCs were labeled with Endorem® as described above, and a cell suspension (at concentrations of 10000, 5000, 2500, 1250, 625, and 315 cells/μL) was suspended in 1.7% gelatin. MR images showed a hypointense signal at all concentrations above 625 cells per μL (Fig. 4a), which means that contrast changes are visible when approximately 70 or more cells are in the nominal pixel (0.055 μL). This minimum concentration of cells for MR visualization applies at the moment of implantation. Subsequent cell divisions in the CNS will serve to decrease the amount of label per cell, and therefore hypointense images at 3–5 weeks postimplantation must necessarily correspond to a much higher cell concentration.

In Vivo MRI Tracking of MSCs

The rats were examined weekly for a period of 3–7 weeks posttransplantation with an MR imager. In lesioned animals prior to grafting, or in lesioned animals subsequently

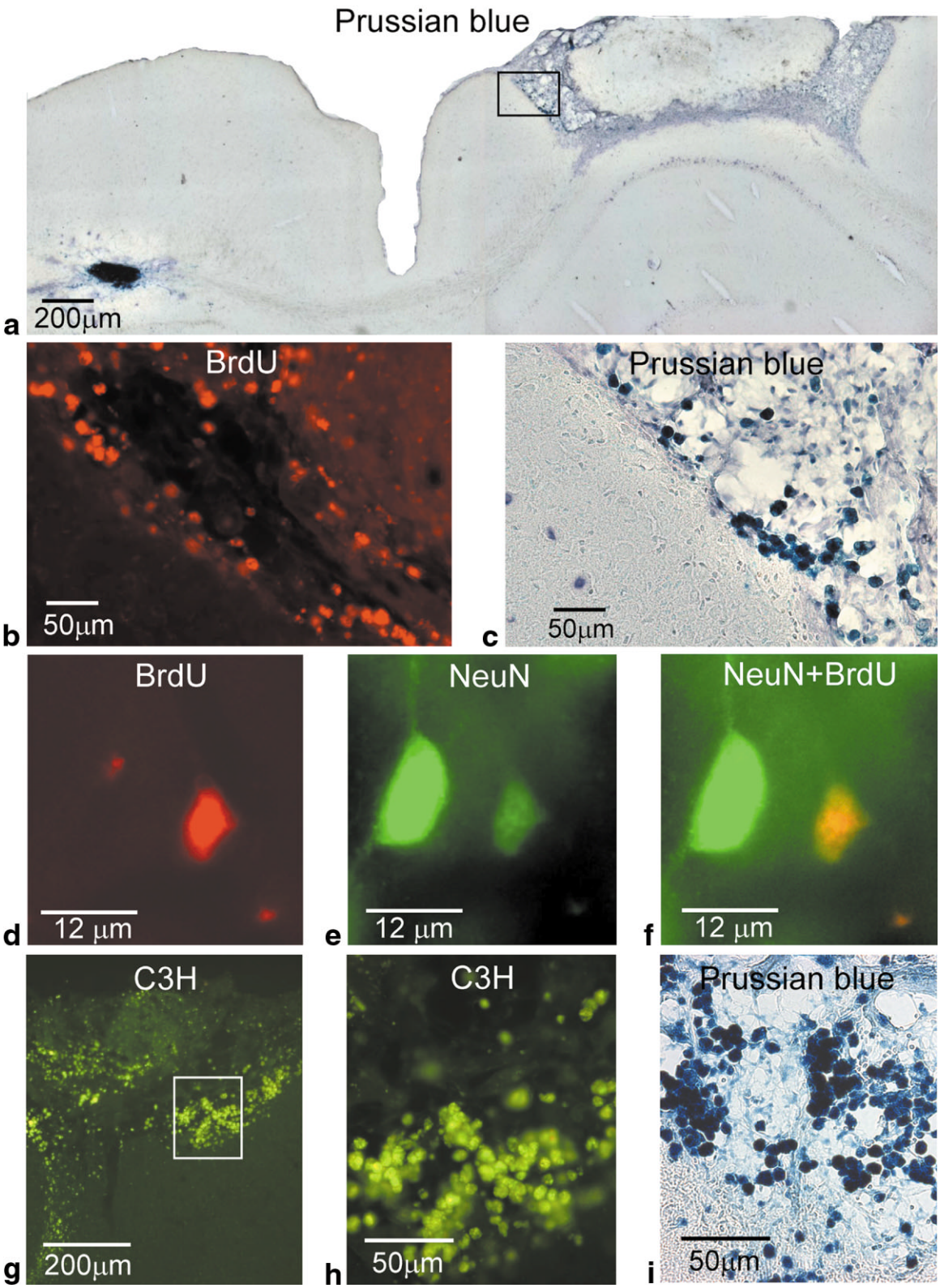

FIG. 2. Intracerebral injection of MSCs into brains with photochemical lesions. **a:** Prussian blue staining of an injection site in the contralateral hemisphere and a photochemical lesion, 4 weeks after grafting. Higher-magnification microphotograph of anti-BrdU staining showing BrdU-positive MSCs in the lesion (**b**) and Prussian blue-stained MSCs on the left edge of the photochemical lesion (**c**). Implanted rat MSCs at the border of the lesion 4 weeks after grafting, double-stained for BrdU (red; **d**) and the neuronal marker NeuN (green; **e**). The coexpression of both markers appears as yellow (**f**). **g–i:** Mouse C3H MSCs labeled with Endorem® migrated into the lesion in the same manner as rat MSCs, 14 days after they were injected into the contralateral hemisphere.

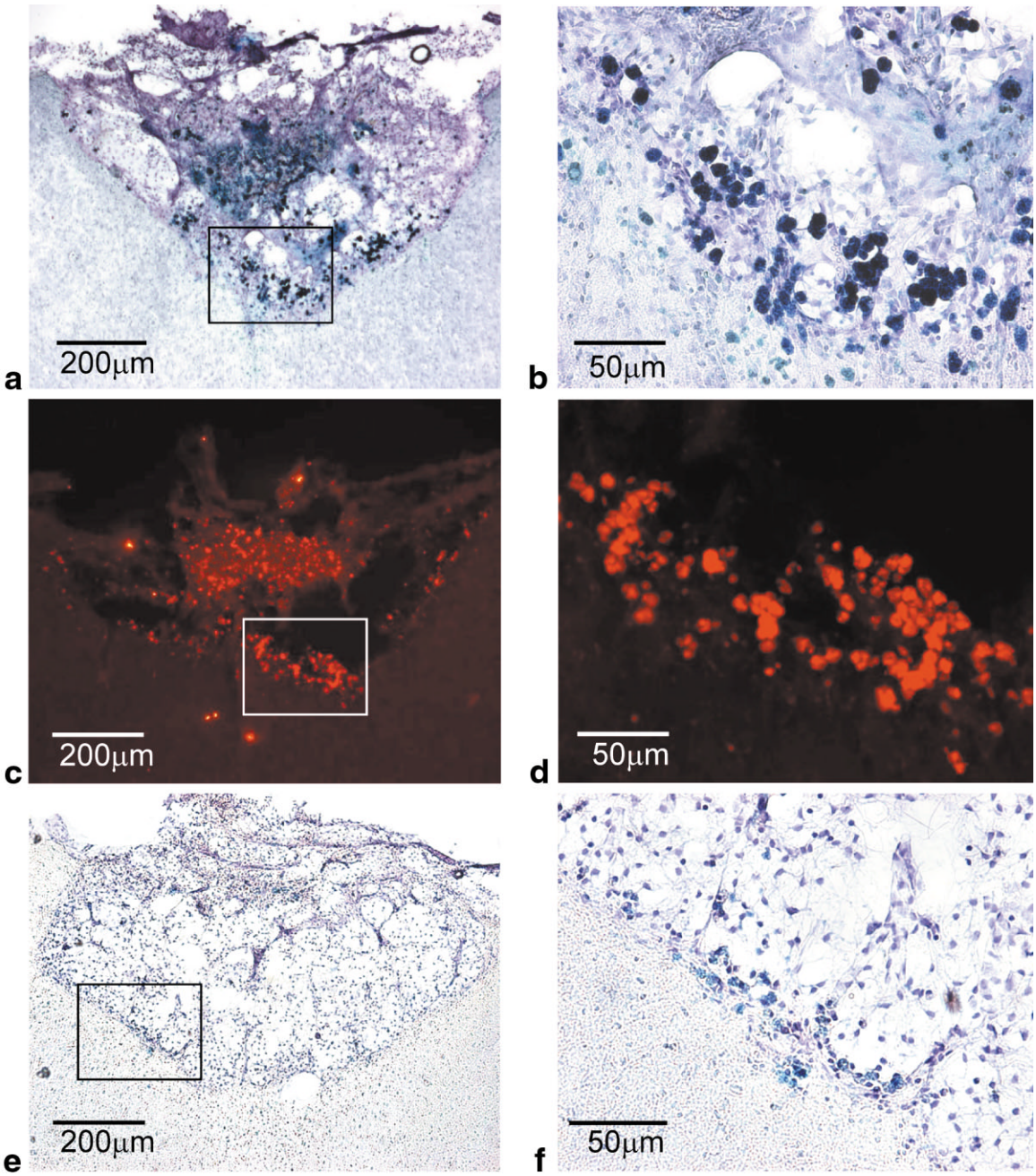

FIG. 3. Intravenous injection of MSCs or PBS into rats with a photochemical lesion. **a** and **b:** Massive invasion of rat MSCs (Prussian blue staining counterstained with hematoxylin) into a photochemical lesion 7 weeks after i.v. injection. **c** and **d:** Serial section stained for BrdU, 7 weeks after i.v. injection. Figures were obtained from the rat brain as shown in Fig. 4c. **e** and **f:** A few weakly stained Prussian blue-positive cells were found in photochemical lesions after intravenous injection of PBS (this section is from an animal that was killed 4 weeks after i.v. injection of PBS).

injected with PBS contralaterally to the lesion (group 5), only the lesion was visible on MR images as a hyperintense signal (Fig. 4b and c). The lesion was clearly visible 2 hr after light exposure; however, after 12–24 hr its borders became sharper and better defined. After 24 hr there were no more changes in the size or shape of the lesion, and it remained visible during the entire measurement period (3–7 weeks).

In rats with a photochemical lesion and cells injected into the contralateral hemisphere (group 2), the cell implants were visible as a hypointense area of approximately 1 mm^2 with sharp borders at the injection site (Fig. 4b). The hypointensity of the cell implant remained visible for the entire 3–7-week period, and the hypointense area did not noticably change in shape. No recognizable hypointense signal in the lesion was detected during the first 2 days after implantation. One week after transplantation, we observed a hypointense signal in the lesion, which intensified during the second and third weeks (Fig. 4b). A weak hypointense signal was also observed in the corpus

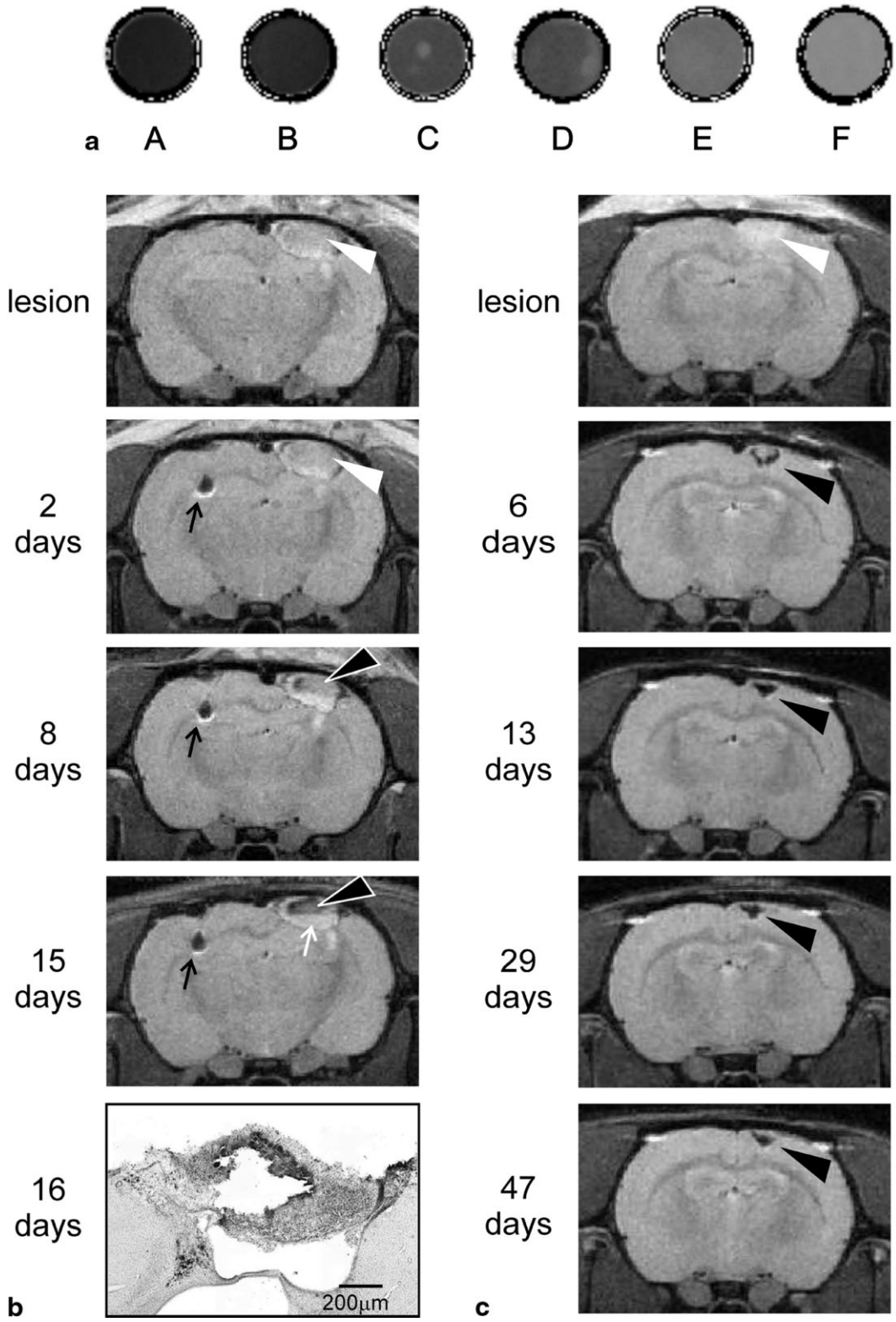

FIG. 4. T_2-weighted images of phantoms and rat brains with a photochemical lesion and implanted MSCs. **a:** MR images of phantoms formed by a set of test tubes containing a suspension of Endorem®-labeled cells in gelatin: (**A**) 10000, (**B**) 5000, (**C**) 2500, (**D**) 1250, and (**E**) 625 cells/μL. Sample **f** contains gelatin only. Inhomogeneities in the phantom images were caused by the moderate sedimentation of cells while the gelatin was setting. **b:** MR images of a cortical photochemical lesion and MSCs implanted into the contralateral hemisphere. **c:** MR images of a cortical photochemical lesion and MSCs injected into the femoral vein. The upper images (lesion) show photochemical lesions (white arrowheads) 12 hr after thrombosis evoked by dye/light interaction, prior to any cell implantation. The cell implant (black arrow) in the hemisphere contralateral to the lesion is clearly visible as a hypointense area (2 days). A hypointense signal in the lesion (black arrowheads) was seen 8 days after grafting and was further enhanced at day 15. Histology performed 16 days postimplantation confirmed a large number of MSCs in the lesion (stained for Prussian blue). Note that the hyperintense area below the lesion (white arrow) seen on day 15 corresponds to the cavity in the damaged tissue (**b**). A hypointense signal (black arrowhead) was observed 6 days after intravenous injection, which was further enhanced 13 days postinjection and persisted for 47 days (**c**).

callosum. At the same time, histology showed that a large number of Prussian blue-positive cells had entered the lesion (Fig. 4b). Many labeled cells were also detected in the corpus callosum, suggesting a migration from the contralateral hemisphere toward the lesion. No hypointense signal was found in other brain regions. The hypointense signal occured only in damaged areas populated with MSCs, and its intensity corresponded to Prussian blue or BrdU staining. Since necrotic parts and subsequent cysts that occurred in some lesions contained interstitial fluid, a weak hyperintense signal was found in these areas of the lesion (see Fig. 4b).

In lesioned rats injected intravenously with MSCs (group 4), we found a hypointense MRI signal only at the site of the lesion (Fig. 4c). The first changes in the hypointensity of the MRI signal in the lesion were observed 6 days after cell injection. The hypointense signal in the lesion reached its maximum at about 2 weeks and persisted with no apparent decrease in signal intensity for about 7 weeks.

DISCUSSION AND CONCLUSIONS

Our study shows that bone marrow stem cells are capable of preferentially migrating into a photochemical lesion. Our results are in agreement with those published by Lu et al. (7,8). In those studies, MSCs were expanded in vitro and administered either intra-arterially or intravenously into rats with a traumatic brain injury. Cells migrated into the injury site, and the transplanted animals showed an improved neurological outcome in behavioral tests. The migration observed in our study was not affected by the route of administration; the lesion was populated with the same number of cells after grafting into the cortex of the contralateral hemisphere as after i.v. injection. Only a small percentage of the cells ($<3\%$) entering the lesion expressed the neuronal marker NeuN. Since we did not perform any electrophysiological studies, we cannot prove that these NeuN-positive cells differentiated into functioning neurons, but in any case their number was very small. We cannot prove that the differentiated MSCs were Endorem®-labeled, since it is not possible to colocalize iron staining and fluorescent NeuN-positive cells. Further experiments examining the differentiation of Endorem®-labeled MSCs would be necessary. In a previous study, Hofstetter et al. (6) induced differentiation with 2-mercaptoethanol and measured the in vitro membrane properties of neuron-like MSCs. The cells in culture did not show typical neuronal properties, such as action potentials or voltage-gated Na^+ and K^+ currents. Nevertheless, the potential usefulness of MSCs in cell therapy does not necessarily rest on the replacement of lost or damaged neurons. Nonhematopoietic bone marrow cells secrete interleukins, stem cell factor, and other hematopoietic regulatory molecules (27,28), including hematopoietic cytokine colony-stimulating factor-1, which is a growth factor in CNS (27). MSCs transplanted into the brain could therefore stimulate tissue regeneration and promote the recovery of function and improve neurological deficits by mechanisms other than direct neuronal replacement (6,8,29). It has been shown that human MSCs in culture respond to extracts from injured brain tissue by producing growth factors such as BDNF, NGF, VEGF, and HGF (30).

To make it feasible to use grafted MSCs in humans, it would be beneficial to find a suitable marker approved for human use that would allow researchers to follow the fate of implanted cells using a noninvasive method. Endorem® is a contrast agent based on dextran-coated superparamagnetic iron-oxide nanoparticles that is clinically approved as a blood pool agent. After it is further tested for cell toxicity, Endorem® may meet the criteria as a cell marker in the CNS. In addition, the use of Endorem® for labeling MSCs does not require any facilitation of iron uptake or cell modification. The iron content of 17.5 pg/cell found in this study is consistent with the findings of Bulte et al. (19), who measured 9–14 pg of iron per cell labeled with magnetodendrimers MD-100. We have demonstrated that MSCs labeled with Endorem® fully retain the ability to divide in vitro and migrate into a lesion in vivo (i.e., they do not behave differently from unlabeled cells). Several types of cells have been examined in studies utilizing different iron-oxide labeling protocols or methodologies for different iron-oxide labeling agents. Bulte et al. (19) developed magnetodendrimers—magnetic tags that can efficiently label human neural stem cells and MSCs through a nonspecific membrane adsorption process with subsequent intracellular localization in endosomes. The mechanism of iron incorporation into the cells was similar to Endorem® cellular uptake; however, in that study human MSCs were labeled only in cell culture, without any grafting or subsequent MR monitoring (19). The same research group reported the neurotransplantation of magnetically labeled oligodendrocyte progenitors by means of MION-46L, which is a dextran-coated nanocolloid with a superparamagnetic maghemite or maghemite-like inverse spinel core structure (18). These magnetic nanoparticles were covalently bound to a monoclonal antibody directed against the transferin receptor. MION-46L alone did not enter oligodendrocyte progenitor cells (18). Grafts of fetal rat tissue prepared as a cell suspension and labeled by incubation with reconstituted Sendai viral envelopes containing iron-oxide particles were studied by Hawrylak et al. (12). They reported that surviving Prussian blue-positive cells with neuron-like morphology were relatively more numerous 10 days after transplantation than at 1–2 months postgrafting. However, the use of viruses for medicinal purposes in humans would raise safety concerns. Modo et al. (20) tracked immortalized stem cells labeled with gadolinium rhodamine dextran transplanted into ischemia-damaged rat hippocampus. This contrast agent is identifiable by both MRI and fluorescence microscopy; however, the MR measurements were done ex vivo, on perfused brains, and did not provide any insight into the dynamic changes in the brain. Recently, cell migration under in vivo conditions was described by Hoehn et al. (21). In that study, embryonic stem cells were labeled by a lipofection procedure with the contrast agent Sinerem® and implanted into ischemic rat brains. However, the lipofection procedure can affect the viability of cells, and the contrast agent Sinerem® has not yet been approved for use in humans.

Histochemical staining for iron (Prussian blue staining) demonstrated the presence of Prussian blue-positive cells in tissue sections in areas that corresponded well to the dark regions in the MRI images. A few iron-containing

Prussian blue-positive cells were occasionally found in the experimental group with a photochemical lesion only (Fig. 3e and f). The iron most likely originated in hemorrhage and iron degradation product release from iron-containing proteins (such as hemoglobin, ferritin, and hemosiderin). The hemorrhage degradation products were probably localized in microglia/macrophages, because macrophages constitute the major cellular pathway for regulating the content and distribution of iron in mammals (31). The lack of any distinct dark region in the images of the nongrafted lesioned brains shows that despite the presence of a few Prussian blue-positive cells seen by histology, the possible presence of iron released from iron-containing proteins did not produce effects as large as those produced by SPIO nanoparticles in the labeled cells. Cadusseau et al. (32) reported the migration of macrophages following the grafting of fetal cell suspensions incubated with lectin-conjugated gold particles. Li et al. (26) observed BrdU uptake into macrophages after transplantation of BrdU-labeled MSCs into ischemic lesions. The macrophages were described as large cells with BrdU present in the cytoplasm, observed mainly in the lesion, while MSCs showed BrdU reactivity localized within the nucleus and were found at the boundary site of the lesion. Similarly, we observed in the lesion a few large flat cells with BrdU-positive spots in the cytoplasm. To rule out any possibility that BrdU uptake into macrophages was responsible for our immunohistochemistry results, we performed the same experiments with mouse C3H MSCs. The pattern of massive migration of mouse C3H MSCs into the lesion was identical to that seen with BrdU-labeled rats MSCs. Thus, we can be certain that nonspecific BrdU uptake into macrophages was not responsible for our staining results.

We conclude that the commercially available contrast agent Endorem® may be useful as a stem cell marker for noninvasive MR tracking of cell fate following transplantation. This study demonstrates that MSCs labeled with iron-oxide nanoparticles remain viable and migrate into an injured site; therefore, this procedure can be used to track implanted cells in experimental animals. These positive results in animals suggest that human trials might be fruitful, after the tolerance of the CNS to Endorem® is verified.

ACKNOWLEDGMENTS

The authors are grateful to Guerbet (Roissy, France) for the generous gift of Endorem®.

REFERENCES

1. Bjorklund A, Lindvall O. Cell replacement therapies for central nervous system disorders. Nat Neurosci 2000;3:537–544.
2. Ourednik V, Ourednik J, Park KI, Snyder EY. Neural stem cells—a versatile tool for cell replacement and gene therapy in the central nervous system. Clin Genet 1999;56:267–278.
3. Svendsen CN, Smith AG. New prospects for human stem-cell therapy in the nervous system. Trends Neurosci 1999;22:357–364.
4. Prockop DJ. Marrow stromal cells as stem cells for nonhematopoietic tissues. Science 1997;276:71–74.
5. Kopen GC, Prockop DJ, Phinney DG. Marrow stromal cells migrate throughout forebrain and cerebellum, and they differentiate into astrocytes after injection into neonatal mouse brains. Proc Natl Acad Sci USA 1999;96:10711–10716.
6. Hofstetter CP, Schwarz EJ, Hess D, Widenfalk J, El Manira A, Prockop JD, Olson L. Marrow stromal cellsform guiding strands in the injured spinal cord and promote recovery. Proc Natl Acad Sci USA 2002;96: 2199–2204.
7. Lu D, Li Y, Wang L, Chen J, Mahmood A, Chopp M. Intraarterial administration of marrow stromal cells in a rat model of traumatic brain injury. J Neurotrauma 2001;18:813–819.
8. Lu D, Mahmood A, Wang L, Li Y, Lu M, Chopp M. Adult bone marrow stromal cells administered intravenously to rats after traumatic brain injury migrate into brain and improve neurological outcome. Neuroreport 2001;12:559–563.
9. Brazelton TR, Rossi FM, Keshet GI, Blau HM. From marrow to brain: expression of neuronal phenotypes in adult mice. Science 2000;290: 1775–1779.
10. Sasaki M, Honmou O, Akiyama Y, Uede T, Hashi K, Kocsis JD. Transplantation of an acutely isolated bone marrow fraction repairs demyelinated adult rat spinal cord axons. Glia 2001;35:26–34.
11. Norman AB, Thomas SR, Pratt RG, Lu SY, Norgren RB. Magnetic resonance imaging of neural transplants in rat brain using a superparamagnetic contrast agent. Brain Res 1992;594:279–283.
12. Hawrylak N, Ghosh P, Broadus J, Schlueter C, Greenough WT, Lauterbur PC. Nuclear magnetic resonance (NMR) imaging of iron oxide-labeled neural transplants. Exp Neurol 1993;121:81–92.
13. Yeh T, Zhang W, Ildstad ST, Ho C. Intracellular labeling of T-cells with superparamagnetic contrast agents. Magn Reson Med 1993;30:617–625.
14. Yeh T, Zhang W, Ildstad ST, Ho C. In vivo dynamic MRI tracking of rat T-cells labeled with superparamagnetic iron-oxide particles. Magn Reson Med 1995;33:200–208.
15. Shen T, Weissleder R, Papisov M, Bogdanov AJ, Brady TJ. Monocrystalline iron oxide nanocompounds (MION): physicochemical properties. Magn Reson Med 1993;29:599–604.
16. Bulte JW, Brooks RA, Moskowitz BM, Bryant LHJ, Frank JA. T1 and T2 relaxometry of monocrystalline iron oxide nanoparticles (MION-46L): theory and experiment. Acad Radiol 1998;5:S137–140.
17. Bulte JW, Brooks RA, Moskowitz BM, Bryant LHJ, Frank JA. Relaxometry and magnetometry of the MR contrast agent MION-46L. Magn Reson Med 1999;42:379–384.
18. Bulte JW, Zhang SC, van Gelderen P, Herynek V, Jordan EK, Duncan ID, Frank JA. Neurotransplantation of magnetically labeled oligodendrocyte progenitors: magnetic resonance tracking of cell migration and myelination. Proc Natl Acad Sci USA 1999;96:15256–15261.
19. Bulte JW, Douglas T, Witwer B, Zhang SC, Strable E, Lewis BK, Zywicke H, Miller B, van Gelderen P, Moskowitz BM, Duncan ID, Frank JA. Magnetodendrimers allow endosomal magnetic labeling and in vivo tracking of stem cells. Nat Biotechnol 2001;19:1141–1147.
20. Modo M, Cash D, Mellodew K, Williams SCR, Fraser SE, Meade TJ, Price J, Hodges H. Tracking transplanted stem cell migration using bifunctional, contrast agent-enhanced, magnetic resonance imaging. NeuroImage 2002;17:803–811.
21. Hoehn M, Kustermann E, Blunk J, Wiedermann D, Trapp T, Focking M, Arnold H, Hescheler J, Fleischmann BK, Buhrle C. Monitoring of implanted stem cell migration in vivo: a highly resolved in vivo magnetic resonance imaging investigation of experimental stroke in rat. Proc Natl Acad Sci USA 2002;100:1073–1078.
22. Bonnemain B. Superparamagnetic and blood pool agents. Spotlight on clinical MRI. Maffliers, France: V.L.C.; 1996. p 75–88.
23. Watson BD, Dietrich WD, Busto R, Wachtel MS, Ginsberg MD. Induction of reproducible brain infarction by photochemically initiated thrombosis. Ann Neurol 1985;17:497–504.
24. Paxinos G, Watson C. The rat brain in stereotaxic coordinates. Sydney: Academic Press; 1986.
25. Michikawa Y, Baba T, Arai Y, Sakakura T, Kusakabe M. Structure and organization of the gene encoding a mouse mitochondrial stress-70 protein. FEBS Lett 1993;1:27–33.
26. Li Y, Chen J, Chen J, Wang L, Lu M, Chopp M. Treatment of stroke in rat with itracarotid administration of marrow stromal cells. Neurology 2001;56:1666–1672.
27. Maysinger D, Berezovskaya O, Fedoroff S. The hematopoietic cytokine colony stimulating factor 1 is also a growth factor in the CNS. II. Microencapsulated CSF-1 and LM-10 cells as delivery systems. Exp Neurol 1996;141:47–56.

28. Eaves CJ, Cashman JD, Kay RJ, Dougherty GJ, Otsuka T, Gaboury LA, Hogge DE, Lansdorp PM, Eaves AC, Humphries RK. Mechanisms that regulate the cell cycle status of very primitive hematopoietic cells in long-term human marrow cultures. II. Analysis of positive and negative regulators produced by stromal cells within the adherent layer. Blood 1991;78:110–117.
29. Li Y, Chopp M, Chen J, Wang L, Gautam SC, Xu YX, Zhang Z. Intrastriatal transplantation of bone marrow nonhematopoietic cells improves functional recovery after stroke in adult mice. J Cereb Blood Flow Metab 2000;20:1311–1319.
30. Chen X, Katakowski M, Li Y, Lu D, Wang L, Zhang L, Chen J, Xu Y, Gautam S, Mahmood A, Chopp M. Human bone marrow stromal cells cultures conditioned by traumatic brain tissue extracts: growth factor production. J Neurosci Res 2002;69:687–691.
31. Brock JH. The biology of iron. In: De Sousa M, Brock JH, editors. Iron in immunity, cancer and inflammation. London: Wiley; 1989. p 35–53.
32. Cadusseau J, Peschanski M. Direct neuronal and macroglial versus indirect macrophage labelling in transplants of fetal neural tissue incubated with gold particles. Exp Neurol 1989;106:265–274.